ORIGINAL PAPER

Analytical determination of the turn-to-turn capacitances for the prediction of voltage peaks in a PWM-fed motor winding

Jan Ole Stockbrügger[1] · Bernd Ponick[1]

Abstract
The number of inverter-fed motors is increasing due to the good controllability of the motor and the meanwhile low acquisition costs. The steep voltage slopes of the converters lead to an uneven voltage distribution along the winding and thus to voltage peaks between the conductors, which stresses the insulation. The voltage distribution can be predicted by means of equivalent circuit diagrams, which take into account the capacitive coupling between the conductors. This paper presents a novel approach for an analytical determination of the turn-to-turn capacitances, which, in addition to the geometry and the placement of the conductors, considers the influence of materials with different permittivities. The conductors are simulated by means of line charges discretely placed inside the electrodes and receptor points attached to the conductor surfaces. The capacitances are determined by means of the Maxwell capacitance matrix. The method is validated by means of FEM simulations for different geometries and materials.

Keywords Turn-to-turn capacitance · Surge voltage distribution · Winding failure · Traction motor · Insulation stress

1 Introduction

An electric machine fed by an inverter has to cope with impressed pulse voltages leading to harmonics of voltage and current, which cause additional oscillating torques and an increased noise level [1]. In order to reduce the negative effects mentioned above, converters with higher switching frequencies have been developed [2]. A high switching frequency of the power electronics is essential, especially for the realization of high-speed drives. An increase in the switching frequency requires a reduction in the switching times of the power semiconductors. Due to the low voltage rise time of the semiconductors, an uneven voltage distribution along the stator winding occurs, which can lead to voltage peaks between the conductors of the winding [3]. The insulation of the electrical machine can be heavily stressed by the voltage peaks and in the worst case, an insulation fault occurs [4]. In order to properly design the insulation, the voltage distribution along the winding must be known. It can be predicted with the help of detailed equivalent electrical

networks, which take into account not only the conductor inductances and resistances but also the capacitive coupling between the conductors [2, 5–9]. The capacitances between conductors are usually determined by means of FEM software [2, 4, 5, 7–9].

Several analytical approximations are based on the equation of a plate capacitance or the method of image charges. In [10], two analytical equations based on the equation of a plate capacitance are compared with FEM simulations to determine the turn-to-turn capacitance of rectangular-shaped conductors. Due to the fact that parallel electrodes are used to derive the equation of a plate capacitance, the corner radius of a rectangular-shaped conductor cannot be taken into account with the analytical equations presented in [10]. The method of image charges is used in [11] to determine the capacitive coupling of round conductors. The conductors are located inside a grounded, cylindrical shield. This method is only suitable for thin conductors because the conductors are only modelled by a single line charge. Otherwise, the near field in the proximity of the conductors is not sufficiently approximated and the surfaces of the conductors do not represent equipotential surfaces [12]. The electrostatic field of a system of conductors placed either above a ground plane or inside a grounded cylinder is calculated in [13] by means of a successive images method. The determination

---

✉ Jan Ole Stockbrügger
ole.stockbruegger@ial.uni-hannover.de

[1] Institute for Drive Systems and Power Electronics, Leibniz University Hannover, Hannover, Germany

of the turn-to-turn capacitance presented in this paper is based on the method described in [14]. In contrast to [14], in which the capacitance between a round conductor and the stator core is determined, no image charges are necessary to determine the considered turn-to-turn capacitances. Furthermore, when calculating the mutual capacitance between conductors, the calculation-intensive determination of the self-capacitance presented in [14] is omitted.

The area to be considered for determining the capacitances between conductors inside a slot is shown in Fig. 1 for round wires and Fig. 2 for rectangular-shaped conductors. The conductors of the stator winding are electrically isolated from the earthed stator by the slot insulation. To insulate the individual conductors from each other, a layer of varnish is applied to each conductor.

As an alternative to computationally expensive FEM simulations, an analytical two-dimensional model for determining the capacitances between conductors is presented below, which considers the contour of the conductors, the distance between the conductors and the medium surrounding the stator winding.

Overall, the calculation model is based on the following simplifications:

- The conductors of the stator winding are ideally electrically conductive.
- There are no space charges within the considered area.
- The medium within the considered geometry consists of a material with constant permittivity.
- The influence of the layer of varnish applied to the conductors and the slot insulation are neglected.

2 Modelling and solution for the field area of round conductors

The field area modelled to determine the turn-to-turn capacitances can be seen in Fig. 3. Nine identical conductors with the radius r_l are present in a medium with the permittivity ε_1, each of the conductors is considered as an electrode for the
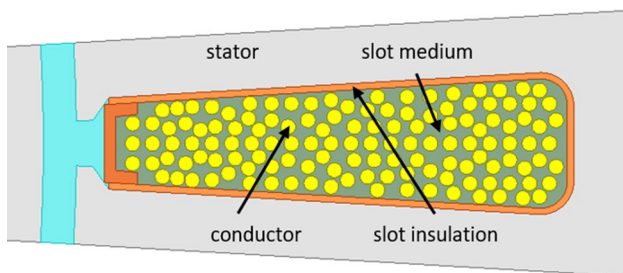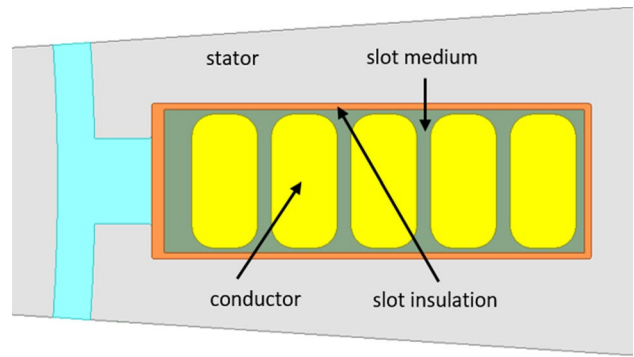

Fig. 2 Example of a slot with rectangular-shaped conductors

field calculation. The conductors can be placed randomly. The nine round conductors l_1 to l_9 have the constant potentials φ_{l1}, φ_{l2}, φ_{l3}, φ_{l4}, φ_{l5}, φ_{l6}, φ_{l7}, φ_{l8} and φ_{l9}.

The capacitive coupling between the centrally arranged conductor l_5 and another conductor in the field area is considered. The neighbouring conductors are used to consider the adjacent round wires in horizontal and in vertical direction. The real conductors are replaced by line charges with the potential

$$\varphi(r) = \frac{\lambda}{2 \cdot \pi \cdot \varepsilon_1} \cdot \ln \left(\frac{1}{|r - \widetilde{r}|} \right)$$
$$= \lambda \cdot \left(\frac{-1}{2 \cdot \pi \cdot \varepsilon_1} \cdot \ln \left(\sqrt{(x - x_\lambda)^2 + (y - y_\lambda)^2} \right) \right). \quad (1)$$

Here, $r = \begin{pmatrix} x & y \end{pmatrix}^T$ is any space vector, in whose coordinates the potential is determined. The position of the line charge is described by the vector $\widetilde{r} = \begin{pmatrix} x_\lambda & y_\lambda \end{pmatrix}^T$. The line charge

Fig. 1 Example of a slot with round conductors
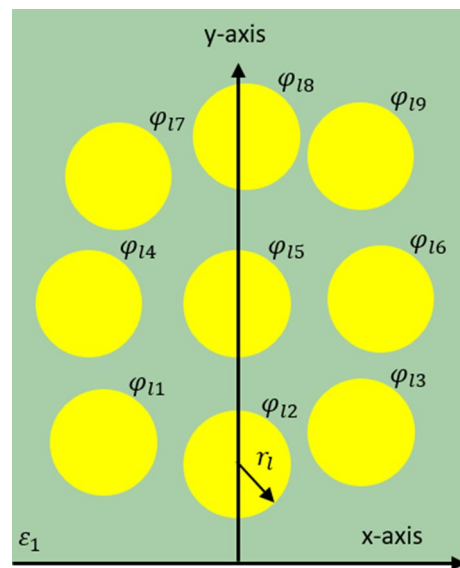

Fig. 3 Exemplary representation of the field area of round conductors

density λ indicates the charge per length. If only one line charge is positioned centrally per conductor, the surfaces of the nine round wires do not represent equipotential surfaces. To determine the near field, the surface charges stored on the conductors are replaced by an integer number of line charges with different line charge densities, which are placed inside the round wires [12]. The unknown line charge densities are determined by means of discrete receptor points placed on the conductor surfaces at those positions, where the specified conductor potentials φ_{l1} to φ_{l9} should be present.

A possible arrangement of the receptor points on the conductor contour and the line charges placed inside the conductors is depicted in Fig. 4.

Each of the nine conductors has W line charges and P receptor points. The P y-coordinates $y_{l,m}$ of the evenly distributed receptor points of the nine conductors are calculated independently of the considered conductor to

$$
\begin{aligned}
y_{l,m} = & r_l \cdot \sin\left(\frac{m \cdot 2 \cdot \pi}{P}\right) \\
& + y_{l,MP} \quad 1 \le l \le 9 \quad 1 \le m \le P
\end{aligned}
\tag{2}
$$

with the y-coordinates of the centre of the considered conductor $y_{l,MP}$ and the integer variables m and l. The P x-coordinates of the receptor points of the conductor $x_{l,m}$ result analogously in

$$
\begin{aligned}
x_{l,m} = & r_l \cdot \cos\left(\frac{m \cdot 2 \cdot \pi}{P}\right) \\
& + x_{l,MP} \quad 1 \le l \le 9 \quad 1 \le m \le P
\end{aligned}
\tag{3}
$$

with the x-coordinate of the centre of the considered conductor $x_{l,MP}$.
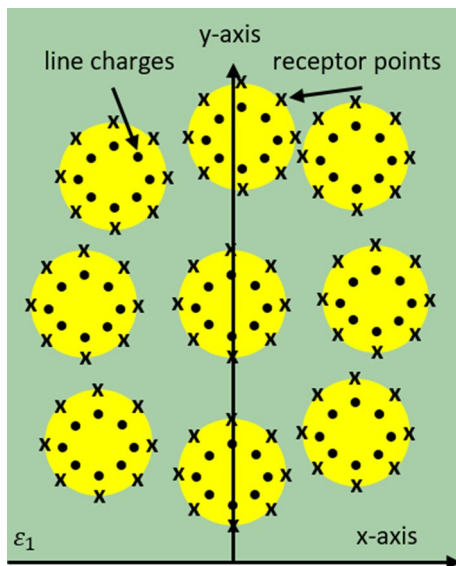

Fig. 4 Placement of line charges and receptor points for round conductors

The W y-coordinates of the line charges of the conductors $y_{\lambda,l,j}$, distributed symmetrically at a radius $F_r \cdot r_l$, $F_r < 1$, inside the conductor are determined to

$$
\begin{aligned}
y_{\lambda,l,n} = & F_r \cdot r_l \cdot \sin\left(\frac{n \cdot 2 \cdot \pi}{W}\right) \\
& + y_{l,MP} \quad 1 \le l \le 9 \quad 1 \le n \le W \quad 0 < F_r < 1.
\end{aligned}
\tag{4}
$$

The W x-coordinates of the line charges of the conductors $y_{\lambda,l,n}$ thus result in

$$
\begin{aligned}
x_{\lambda,l,n} = & F_r \cdot r_l \cdot \cos\left(\frac{n \cdot 2 \cdot \pi}{W}\right) \\
& + x_{l,MP} \quad 1 \le l \le 9 \quad 1 \le n \le W.
\end{aligned}
\tag{5}
$$

At the positions of the total $9P$ receptor points, the potential can be calculated as a function of the $9W$ line charges using (1) to

$$
\phi = \begin{pmatrix} \varphi(x_{1,1}, y_{1,1}) \\ \varphi(x_{1,2}, y_{1,2}) \\ I \ldots \\ \varphi(x_{9,P}, y_{9,P}) \end{pmatrix} = A \cdot \begin{pmatrix} \lambda_1 \\ \lambda_2 \\ \ldots \\ \lambda_{9W} \end{pmatrix}
$$
$$
= A \cdot \lambda \quad A \epsilon M^{(9P) \times (9W)}.
\tag{6}
$$

The coefficient matrix A describes the influence of the line charges on the potentials in the receptor points and contains in each element the second factor of (1) depending on the addressed receptor point and the addressed line charge.

The potentials of the receptor points ϕ result from the required potentials of the conductor potentials at

$$
\phi(u) = \begin{cases} \varphi_{l1} & \text{for } 1 \le u \le P \\ \varphi_{l2} & \text{for } P < u \le 2P \\ \varphi_{l3} & \text{for } 2P < u \le 3P \\ \varphi_{l4} & \text{for } 3P < u \le 4P \\ \varphi_{l5} & \text{for } 4P < u \le 5P \quad 1 \le u \le 9P \\ \varphi_{l6} & \text{for } 5P < u \le 6P \\ \varphi_{l7} & \text{for } 6P < u \le 7P \\ \varphi_{l8} & \text{for } 7P < u \le 8P \\ \varphi_{l9} & \text{for } 8P < u \le 9P \end{cases}
\tag{7}
$$

with the integer running variable u.

A clearly solvable system of equations is achieved with the same number of line charges and receptor points. With the help of the pseudoinverse of the coefficient matrix A^{-1}, the unknown line charge densities are determined as

$$
\lambda = A^{-1} \cdot \phi.
\tag{8}
$$

The determination of the scalar potential field in the medium outside the round conductors finally results from the superposition of the corresponding values of the potentials of the $9W$ line charges according to (1).

3 Calculation of the phase-to-phase capacitance of round conductors

The capacitance between the centrally placed conductor l_5 and the conductor l_i C_{l5li} is determined with the aid of the Maxwell capacitance coefficients, with which the concept of capacitance can be applied to systems consisting of several electrodes insulated from each other [15]. In this problem definition, the nine conductors with the charge λ_l and the potential φ_l are considered as electrodes. The corresponding capacitance coefficient matrix is

$$
\begin{pmatrix} \lambda_{l1} \\ \lambda_{l2} \\ \lambda_{l3} \\ \lambda_{l4} \\ \lambda_{l5} \\ \lambda_{l6} \\ \lambda_{l7} \\ \lambda_{l8} \\ \lambda_{l9} \end{pmatrix} = \begin{pmatrix} c_{l1l1} & c_{l1l2} & c_{l1l3} & c_{l1l4} & c_{l1l5} & c_{l1l6} & c_{l1l7} & c_{l1l8} & c_{l1l9} \\ c_{l2l1} & c_{l2l2} & c_{l2l3} & c_{l2l4} & c_{l2l5} & c_{l2l6} & c_{l2l7} & c_{l2l8} & c_{l2l9} \\ c_{l3l1} & c_{l3l2} & c_{l3l3} & c_{l3l4} & c_{l3l5} & c_{l3l6} & c_{l3l7} & c_{l3l8} & c_{l3l9} \\ c_{l4l1} & c_{l4l2} & c_{l4l3} & c_{l4l4} & c_{l4l5} & c_{l4l6} & c_{l4l7} & c_{l4l8} & c_{l4l9} \\ c_{l5l1} & c_{l5l2} & c_{l5l3} & c_{l5l4} & c_{l5l5} & c_{l5l6} & c_{l5l7} & c_{l5l8} & c_{l5l9} \\ c_{l6l1} & c_{l6l2} & c_{l6l3} & c_{l6l4} & c_{l6l5} & c_{l6l6} & c_{l6l7} & c_{l6l8} & c_{l6l9} \\ c_{l7l1} & c_{l7l2} & c_{l7l3} & c_{l7l4} & c_{l7l5} & c_{l7l6} & c_{l7l7} & c_{l7l8} & c_{l7l9} \\ c_{l8l1} & c_{l8l2} & c_{l8l3} & c_{l8l4} & c_{l8l5} & c_{l8l6} & c_{l8l7} & c_{l8l8} & c_{l8l9} \\ c_{l9l1} & c_{l9l2} & c_{l9l3} & c_{l9l4} & c_{l9l5} & c_{l9l6} & c_{l9l7} & c_{l9l8} & c_{l9l9} \end{pmatrix} \cdot \begin{pmatrix} \varphi_{l1} \\ \varphi_{l2} \\ \varphi_{l3} \\ \varphi_{l4} \\ \varphi_{l5} \\ \varphi_{l6} \\ \varphi_{l7} \\ \varphi_{l8} \\ \varphi_{l9} \end{pmatrix}.
$$
(9)

The resulting charges of the nine round conductors λ_{l1}, λ_{l2}, λ_{l3}, λ_{l4}, λ_{l5}, λ_{l6}, λ_{l7}, λ_{l8} and λ_{l9} can be determined according to (8) by a division of the vector λ and a subsequent summation of the line charges placed within the individual conductors to

$$
\lambda_{lj} = \sum_{i=1+P\cdot(j-1)}^{j\cdot P} \lambda_i \quad 1 \le j \le 9
$$
(10)

with the integer variable j. The capacitance coefficients $c_{\mu v}$ correspond to the capacitances $C_{\mu v}$ in the case of counter-capacitances $\mu \ne v$, which establish a connection between the charges and the potential differences.

By selecting a conductor potential of zero volts with the exception of conductor l_i, according to (9), the capacitance between conductors yields

$$
C_{l5li} = l_{fe} \cdot c_{l5li} = l_{fe} \cdot \frac{\lambda_{l5}}{\varphi_i}
$$
(11)

with the core length of the electrical machine l_{fe}.

4 Modelling and solution for the field area of rectangular-shaped conductors

The field area modelled to determine the turn-to-turn capacitances can be seen in Fig. 5. Three identical rectangular-shaped conductors, which are considered as electrodes here, with the defined corner radius r_e are located in the medium with the permittivity ε_1. The field area is limited in y-direction by the stator lamination with the potential φ_s. Based on
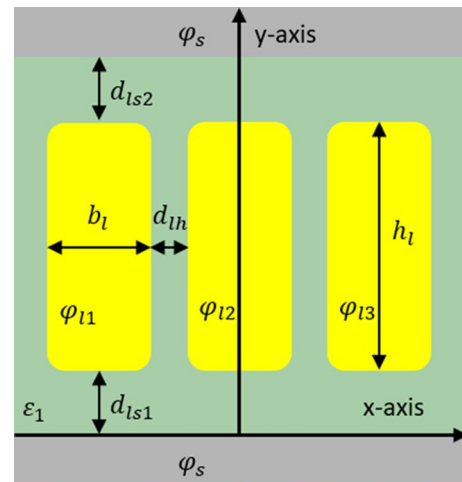

Fig. 5 Representation of the field area of rectangular-shaped conductors

the vertical distances between the conductors and the stator lamination d_{ls1} and d_{ls2}, an asymmetrical placement of the electrodes within the slot can be considered.

The three electrodes are evenly distributed in x-direction. The horizontal distance between adjacent conductors is d_{lh}. The rectangular-shaped conductors l_1, l_2 and l_3 are described by their width b_l and their height h_l and have the constant potentials φ_{l1}, φ_{l2} and φ_{l3}. The capacitive coupling of the conductor l_2 in the middle is considered.

The procedure for solving the field area is taken from Sect. 2. A possible arrangement of the receptor points placed on the electrode surfaces, at whose positions the specified conductor potentials φ_{l1}, φ_{l2} and φ_{l3} and the stator potential φ_s, respectively, should be present, can be taken from Fig. 6. For a reproduction of the corner radii, the placement of receptor points on the circular sections of the rectangular-shaped conductors is necessary.

The line charges are placed inside the conductors and inside the stator lamination. The lamination parts above and below the rectangular-shaped conductors represent one electrode each. For mathematical differentiation, the upper lamination electrode has the potential φ_{s1} and the lower lamination electrode the potential φ_{s2}.

The height of the electrodes has no influence on the turn-to-turn capacitances. The width of the considered lamination electrodes in y-direction is selected so that there is a vertical limitation in the field area between the three rectangular-shaped conductors.

Each of the five electrodes has W line charges and P receptor points. At the position of the total of $5P$ receptor points, the potential can be calculated as a function of the $5W$ line charges using (1) to
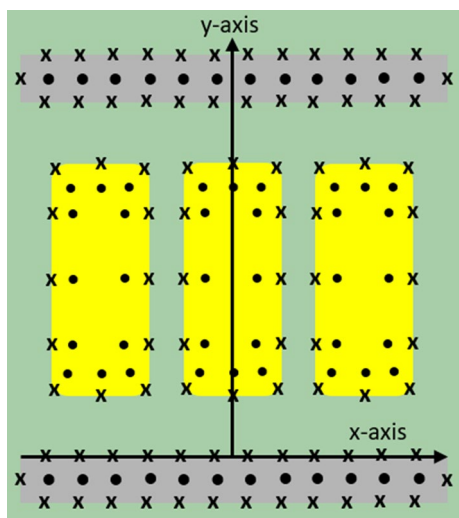
Fig. 6 Placement of line charges and receptor points for rectangular-shaped conductors

$$\phi = \begin{pmatrix} \varphi(x_{1,1}, y_{1,1}) \\ \varphi(x_{1,2}, y_{1,2}) \\ I \dots \\ \varphi(x_{5,P}, y_{5,P}) \end{pmatrix} = A \cdot \begin{pmatrix} \lambda_1 \\ \lambda_2 \\ \dots \\ \lambda_{5W} \end{pmatrix} \qquad (12)$$

$$= A \cdot \lambda \quad A \epsilon M^{(5P)x(5W)}.$$

The potentials of the receptor points ϕ are calculated using the integer variable u to

$$\phi(u) = \begin{cases} \varphi_{l1} & \text{für } 1 \leq u \leq P \\ \varphi_{l2} & \text{für } P < u \leq 2P \\ \varphi_{l3} & \text{für } 2P < u \leq 3P \quad 1 \leq u \leq 5P. \\ \varphi_{s1} & \text{für } 3P < u \leq 4P \\ \varphi_{s2} & \text{für } 4P < u \leq 5P \end{cases} \qquad (13)$$

The unknown line charge densities are determined using the pseudoinverse of the coefficient matrix A^{-1} by

$$\lambda = A^{-1} \cdot \phi. \qquad (14)$$

The determination of the scalar potential field in the medium between the conductors is finally obtained by superposition of the corresponding values of the potentials of the $5W$ line charges according to (1).

5 Calculation of the turn-to-turn capacitances of rectangular-shaped conductors

The determination of the capacitances between the conductor in the middle and the adjacent conductor l_i C_{l2li} is carried out analogously to the procedure described in Sect. 3. The capacitance coefficient matrix for the field area shown in Fig. 6 is

$$\begin{pmatrix} \lambda_{l1} \\ \lambda_{l2} \\ \lambda_{l3} \\ \lambda_{s1} \\ \lambda_{s2} \end{pmatrix} = \begin{pmatrix} c_{l1l1} & c_{l1l2} & c_{l1l3} & c_{l1s1} & c_{l1s2} \\ c_{l2l1} & c_{l2l2} & c_{l2l3} & c_{l2s1} & c_{l2s2} \\ c_{l3l1} & c_{l3l2} & c_{l3l3} & c_{l3s1} & c_{l3s2} \\ c_{s1l1} & c_{s1l2} & c_{s1l3} & c_{s1s1} & c_{s1s2} \\ c_{s2l1} & c_{s2l2} & c_{s2l3} & c_{s2s1} & c_{s2s2} \end{pmatrix} \cdot \begin{pmatrix} \varphi_{l1} \\ \varphi_{l2} \\ \varphi_{l3} \\ \varphi_{s1} \\ \varphi_{s2} \end{pmatrix} \qquad (15)$$

The resulting charges of the three rectangular-shaped conductors λ_{l1}, λ_{l2} and λ_{l3} can be determined according to (14) by dividing the vector λ into

$$\lambda_{lj} = \sum_{i=1+P \cdot (j-1)}^{j \cdot P} \lambda_i \qquad \leq j \leq 3. \qquad (16)$$

By selecting a conductor and a stator lamination potential of zero volts with the exception of conductor l_i, according to (15) the turn-to-turn capacitance results in

$$C_{l2li} = l_{fe} \cdot c_{l2li} = l_{fe} \cdot \frac{\lambda_{l2}}{\varphi_i}. \qquad (17)$$

To determine the capacitance between rectangular-shaped conductors in the end winding region of an electrical machine, the two lamination electrodes contained in Fig. 6 are removed from the field area and the calculation is done again with three electrodes only.

6 Validation of the model

The validation of the models is carried out separately for round wires and rectangular-shaped conductors by means of FEM simulations. The six investigated machine variants with round wires, which differ in their geometries and material properties, are summarized in Table 1. The first three variants represent a random placement of the conductors as shown in Fig. 3. The fourth, fifth and sixth variants simulate an orthocyclic winding. An exemplary representation of the field area is shown in Fig. 7. The nine round conductors are represented by 36 receptor points and 36 line charges each. The reduction factor is $F_r = 0.9$ for all conductors.

Table 2 contains the analytically calculated and Table 3 the numerically determined capacitances between round conductors.

The deviations between the analytical model and the FEM simulations shown in Table 4 are in the low percentage range. The errors in the analytical solution are due to the finite number of receptor points and line charges. In addition, deviations in the numerical solution are caused by the limitation of the medium in the x and the y direction with Neumann boundary conditions.

Table 1 Geometric and material properties of the investigated round conductor models

	Variant 1	Variant 2	Variant 3	Variant 4	Variant 5	Variant 6
r_l in mm	0.30	0.60	0.60	0.90	0.90	1.20
$x_{1.MP}$ in mm	−0.80	−1.50	−1.30	0.00	0.00	0.00
$y_{1.MP}$ in mm	0.40	0.50	1.30	2.35	−0.58	−0.80
$x_{2.MP}$ in mm	0.00	0.00	−0.05	−0.99	−0.97	−1.30
$y_{2.MP}$ in mm	0.35	0.50	0.65	4.25	1.25	1.80
$x_{3.MP}$ in mm	0.88	1.70	1.35	0.975	0.97	1.30
$y_{3.MP}$ in mm	0.50	0.90	0.65	4.25	1.25	1.80
$x_{4.MP}$ in mm	−0.80	−1.55	−1.75	−1.95	−1.94	−2.60
$y_{4.MP}$ in mm	1.11	2.25	2.55	6.15	3.08	4.40
$x_{5.MP}$ in mm	0.00	0.00	−0.10	0.00	0.00	0.00
$y_{5.MP}$ in mm	1.11	2.10	2.50	6.15	3.08	4.40
$x_{6.MP}$ in mm	0.85	1.25	1.30	1.95	1.94	2.60
$y_{6.MP}$ in mm	1.20	2.10	2.20	6.15	3.08	4.40
$x_{7.MP}$ in mm	−0.85	−1.55	−1.25	−0.99	−0.97	−1.30
$y_{7.MP}$ in mm	1.75	3.75	4.10	8.05	4.91	7.00
$x_{8.MP}$ in mm	0.00	0.00	0.30	0.98	0.97	1.30
$y_{8.MP}$ in mm	1.85	3.40	3.75	8.05	4.91	7.00
$x_{9.MP}$ in mm	0.65	1.75	1.60	0.00	0.00	0.00
$y_{9.MP}$ in mm	1.80	3.70	3.50	9.95	6.74	9.60
ε_{r1}	5.20	1.00	3.17	1.00	5.2	3.17
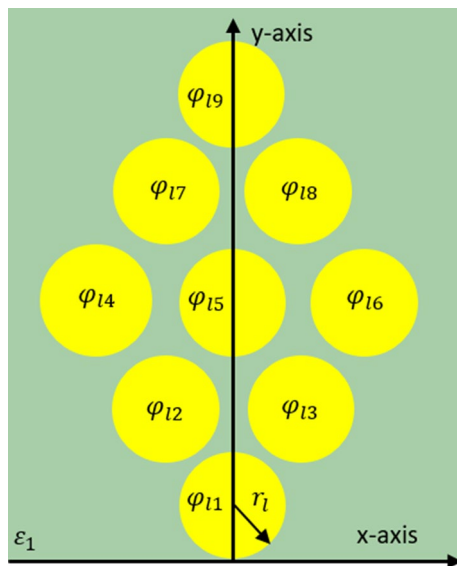
Fig. 7 Representation of the field area of orthocyclic winding

The highest deviations in the investigation of the fourth and sixth variants are found for the turn-to-turn capacitances with the lowest values. Here, capacitive coupling can be almost neglected due to the low capacitance.

The six investigated machine variants with rectangular-shaped conductors can be seen in Table 5. The FEM model structure corresponds to the field area shown in Fig. 5. The three rectangular-shaped conductors and the two stator sections are each represented by 100 receptor points and 100 line charges.

Table 6 shows the analytically calculated and numerically determined capacitances between rectangular-shaped conductors. Due to the identical spacing between the first and second and the second and third rectangular-shaped conductor, the capacitance C'_{l2l1} corresponds to the capacitance C'_{l2l3}. The deviations are in the single-digit percentage range. The errors in the analytical solution can be explained by the finite number and the placement of the receptor points and the line charges. In addition, deviations in the numerical solution result from the limitation of the media with Neumann boundary conditions.

In order to demonstrate the quality of the novel analytical approach proposed in this paper, Table 7 contains the length-related capacitances between rectangular-shaped conductors $C'_{l2li,pk}$ which are analytically determined using the simple equation for a plate capacitor. Instead of the novel approach the height of the plate capacitor corresponds to the side length of the rectangular-shaped conductor including the corner radii.

Only in case the distance between the rectangular-shaped conductors is small and the corner radius is small compared to the side length of the rectangular-shaped conductor, as it is the case for variant 5 and 6, the capacitance between rectangular-shaped conductors can be approximated by means of a plate capacitor. In this case, the varnish insulation can be considered as an additional single-layer plate capacitor.

Table 2 Analytically calculated, length-related capacitances between round conductors C'_{l5li}

Capacitance in pF/m	Variant 1	Variant 2	Variant 3	Variant 4	Variant 5	Variant 6
C'_{l5l1}	11.99	2.64	36.97	6.22e−5	6.49e−5	5.18e−4
C'_{l5l2}	128.06	18.27	27.43	21.84	138.30	63.31
C'_{l5l3}	17.73	1.35	2.75	22.38	138.30	63.31
C'_{l5l4}	94.08	20.26	45.49	46.66	248.79	150.26
C'_{l5l6}	68.51	79.96	90.30	46.65	248.79	150.26
C'_{l5l7}	11.32	0.68	14.71	21.84	138.30	63.31
C'_{l5l8}	121.48	51.57	151.92	22.38	138.30	63.31
C'_{l5l9}	21.15	0.34	3.76	6.22e−5	6.49e−5	5.18e−4

Table 3 Numerically determined, length-related capacitances between round conductors C'_{l5li}

Capacitance in pF/m	Variant 1	Variant 2	Variant 3	Variant 4	Variant 5	Variant 6
C'_{l5l1}	11.58	2.63	36.62	5.45e−5	6.59e−5	4.73e−4
C'_{l5l2}	119.98	18.05	27.21	21.43	135.19	62.23
C'_{l5l3}	17.23	1.35	2.76	21.96	135.19	62.23
C'_{l5l4}	92.94	20.01	45.01	45.06	239.66	145.16
C'_{l5l6}	68.01	75.47	88.76	45.06	239.66	145.16
C'_{l5l7}	11.69	0.68	14.64	21.43	135.19	62.23
C'_{l5l8}	126.61	49.91	147.45	21.96	135.19	62.23
C'_{l5l9}	21.74	0.34	3.77	5.45e−5	6.43e−5	4.73e−4

Table 4 Percentage deviations between analytically calculated and numerically determined capacitances between round conductors C'_{l5li}

Deviation in %	Variant 1	Variant 2	Variant 3	Variant 4	Variant 5	Variant 6
C'_{l5l1}	3.54	0.38	0.96	14.13	1.52	9.51
C'_{l5l2}	6.73	1.22	0.81	1.91	2.30	1.74
C'_{l5l3}	2.90	0.00	0.36	1.91	2.30	1.74
C'_{l5l4}	1.23	1.25	1.07	3.55	3.81	3.51
C'_{l5l6}	0.74	5.95	1.74	3.53	3.81	3.51
C'_{l5l7}	3.17	0.00	0.48	1.91	2.30	1.74
C'_{l5l8}	4.05	3.33	3.03	1.91	2.30	1.74
C'_{l5l9}	2.71	0.00	0.27	14.13	0.93	9.51

Table 5 Geometric and material properties of the investigated rectangular-shaped conductor models

Variant	r_e in mm	d_{ls1} in mm	d_{ls2} in mm	d_{lh} in mm	h_l in mm	b_l in mm	ε_{r1}
1	0.65	0.225	0.225	0.145	4.75	1.66	1.00
2	0.50	0.325	0.425	0.145	4.75	1.66	1.00
3	0.30	0.50	1.00	0.20	5.00	2.00	3.20
4	0.60	0.45	0.55	0.30	4.50	3.00	3.20
5	0.10	0.45	0.45	0.10	3.00	1.00	5.00
6	0.80	1.00	2.00	0.50	6.00	3.00	5.00

7 Conclusion

This paper presents a simple and fast analytical calculation method for the turn-to-turn capacitances. The determination is based on the field solution for a two-dimensional area. The round conductors and the rectangular-shaped conductors are modelled by a finite number of discrete receptor points and discrete line charges. The

Table 6 Comparison of the analytically calculated, length-related capacitances between rectangular-shaped conductors C'_{l2li} with the FEM results

Variant	$C'_{l2li\cdot anal}$ in pF/m	$C'_{l2li\cdot FEM}$ in pF/m	Deviation C'_{l2li} in %
1	250.45	247.34	1.26
2	264.66	262.45	0.84
3	699.73	691.68	1.16
4	388.32	384.87	0.90
5	1344.30	1342.80	0.11
6	507.71	503.26	0.88

Table 7 Comparison of the length-related capacitances between rectangular-shaped conductors analytically calculated using the equation for a plate capacitor C'_{l2s} with the FEM results

Variant	$C'_{l2li\cdot pk\cdot anal}$ in pF/m	$C'_{l2li\cdot FEM}$ in pF/m	Deviation C'_{l2li} in %
1	369.43	247.34	49.36
2	351.11	262.45	33.78
3	793.34	691.68	14.70
4	538.33	384.87	39.87
5	1416.70	1342.80	5.50
6	508.20	503.26	0.98

determination of the counter-capacitances is carried out with the help of the Maxwell capacitance coefficients and the given electrode potentials. The validation with the help of FEM simulations confirms the applicability of the proposed method.

With the help of the presented approach, the effect of different geometries and materials on the turn-to-turn capacitances can be determined.

Due to the use of line charges within the electrodes, the method can also be used for other conductor geometries.

Compliance with ethical standards

Conflict of interest The authors declare that they have no conflict of interest.

Availability of data and material Available.

Code availability Available.

References

1. Berth M (1998) Elektrische Belastung der Wicklungsisolierung pulsumrichtergespeister Niederspannungsmotoren, Fortschritt-Berichte VDI, Reihe 21: Elektrotechnik, Band 247, VDI
2. Hwang D, Lee K, Jeon J, Kim Y, Kim M, Kim D (2005) Analysis of voltage distribution in stator winding of IGBT PWM inverter-fed induction motors. In: IEEE international symposium on industrial electronics, Dubrovnik, vol 3, pp 945–950
3. Xie Y, Zhang J, Leonardi F, Munoz A, Degner M, Liang F (2019) Voltage Stress Modeling and Measurement for Random-Wound Windings Driven by Inverters. In: IEEE international electric machines and drives conference, San Diego, pp 1917–1924
4. Venegas V, Escarela R, Mota R, Melgoza E, Guardado J (2003) Calculation of electrical parameters for transient overvoltage studies on electrical machines. In: IEEE international electric machines and drives conference, Madison, vol 3, pp 1978–1982.
5. Mihaila V, Duchesne S, Roger D (2011) A simulation method to predict the turn-to-turn voltage spikes in a PWM fed motor winding. IEEE Trans Dielectr Electr Insul 18(5):1609–1615
6. Guardado J, Cornick K (1996) Calculation of machine winding electrical parameters at high frequencies for switching transient studies. IEEE Trans Energy Convers 11(1):33–40
7. Mihaila V, Duchesne S, Roger D, Liegeois P (2011) Prediction of the turn-to-turn voltages in parallel connected wires configuration for motor coils fed by steep fronted pulses. In: Electrical insulation conference, Annapolis, pp 407–412
8. Jianru W, Yangjian S, Xianbin X (2004) Research on nonuniform voltage distribution in winding turns of motor driven by high frequency pulse. In: 4th international power electronics and motion control conference, Xi'an, vol 2, pp 563–567
9. Ferreira R, Ferreira A (2018) Transient voltage distribution in induction motor stator windings using finite elements method. IEEE Ind Electron Soc, Washington, pp 737–742
10. Djukic N, Encica L, Paulides JJH (2016) Electrical machines: Comparison of existing analytical models and FEM for calculation of turn-to-turn capacitance in formed windings. In: International conference on ecological vehicles and renewable energies, Monte Carlo
11. Zhang S (1994) Calculation of the partial capacitance in a system of conductors within the calculable resistor. IEEE Trans Instrum Measur 43(6):929–932
12. Scheible J (1991) Die Lösung des feldtheoretischen Viermedienproblems ebener Schichten. Arch für Elektrotechnik 75:9–17
13. Sarma M, Janischewskyj W (1969) Electrostatic field of a system of parallel cylindrical conductors. IEEE Trans Power Appar Syst PAS-88(7):1069–1079
14. Stockbrügger J.O, Ponick, B (2020) Analytische Ermittlung der Wicklung-Stator-Kapazität in elektrischen Maschinen zur Vorausberechnung des hochfrequenten Common-Mode-Stroms, e & i Elektrotechnik und Informationstechnik
15. Küpfmüller K, Mathis W, Reibiger A (2013) Theoretische Elektrotechnik, 19th edn. Springer, Heidelberg